Title

Energy, economic, and environmental analysis of integration of thermal energy storage into district heating systems using waste heat from data centres

Authors

Li, Haoran

Hou, Juan

Hong, Tianzhen

et al.

Publication Date

2021-03-01

DOI

10.1016/j.energy.2020.119582

Peer reviewed

Energy 219 (2021) 119582

Contents lists available at ScienceDirect

Energy

journal homepage: www.elsevier.com/locate/energy

Energy, economic, and environmental analysis of integration of thermal energy storage into district heating systems using waste heat from data centres

Haoran Li [a, *], Juan Hou [a], Tianzhen Hong [b], Yuemin Ding [a], Natasa Nord [a]

[a] Department of Energy and Process Technology, Norwegian University of Science and Technology (NTNU), Kolbjørn Hejes Vei 1 B, Trondheim, 7491, Norway
[b] Building Technology and Urban Systems Division, Lawrence Berkeley National Laboratory, One Cyclotron Road, Berkeley, CA, 94720, USA

ARTICLE INFO

Article history:
Received 28 April 2020
Received in revised form
7 December 2020
Accepted 9 December 2020
Available online 16 December 2020

Keywords:
Mismatch problem
Peak load
Borehole thermal energy storage
Water tank
Energy bill
CO_2 emissions

ABSTRACT

Data centres produce waste heat, which can be utilized in district heating systems. However, the mismatch between data centres' heat supply and district heating systems' heat demands limits its utilization. Further, high peak loads increase the operation cost of district heating systems. This study aimed to solve these problems by introducing thermal energy storages. A water tank and a borehole thermal energy storage system were selected as the short-term and long-term thermal energy storage, respectively. Energy, economic, and environmental indicators were introduced to evaluate different solutions. The case study was a campus district heating system in Norway. Results showed that the water tank could shave the peak load by 31% and save the annual energy cost by 5%. The payback period was lower than 15 years when the storage efficiency remained higher than 80%. However, it had no obvious benefits in terms of mismatch relieving and CO_2 emissions reduction. In contrast, the borehole thermal energy storage increased the waste heat utilization rate to 96% and reduced the annual CO_2 emissions by 8%. However, the payback period was more than 17 years. These results provide guidelines for the retrofit of district heating systems, where data centres' waste heat is available.

1. Introduction

The fundamental idea of district heating (DH) is to utilise local resources that would otherwise be wasted to satisfy local heat demand [1]. Suitable resources include waste incineration, geothermal energy, solar thermal energy, and waste heat [2–8]. Among these, waste heat plays an important role in current DH systems. In the countries of the European Union, about 72% of the heat supply comes from waste heat [9]. Moreover, the current DH systems are facing a transformation to the fourth generation DH, which will decrease temperature levels dramatically. The decrease in temperature will bring huge potential for waste heat utilization in DH systems [10–14].

Waste heat can come from industrial processes, combined heat and power plants, and large electricity users [15–17]. Waste heat from data centres (DCs) is a promising heat resource, especially for the Nordic countries [18]. First, DCs are energy-intensive facilities and the amounts of electricity used globally by DCs have grown significantly in recent years. Up to 2010, DCs accounted for 1.3% of the world's electricity use. However, this proportion is increasing, with an annual growth rate of 25% [19]. Second, a large proportion of this electricity is converted into waste heat [20,21]. For a typical DC, about half of the electricity used ultimately becomes waste heat. Third, the equally spread load profile and waste heat generation make DCs a reliable heat source [17]. Finally, many DCs are built close to an existing DH network. Therefore, it is possible to feed the DCs' waste heat into the nearby DH networks [18].

Studies have showed that it is technically and economically feasible to recycle waste heat for DH systems usage. According to a review by Ebrahimi et al., techniques for recycling waste heat from a DC include absorption cooling, electricity generation, and DH [22]. Wahlroos et al. studied one Finnish DH system with waste heat recovery from a DC. The results showed that operation cost savings of 0.6–7.3% could be made after recycling waste heat from the DC [17]. Similarly, Davies et al. investigated a DH system in London. The results showed that waste heat recovery from a DC reduced the annual operational cost by $373,634-$876,000 [23]. Kauko et al. studied a Norwegian DH system. Their results showed that heat

* Corresponding author.
E-mail address: haoranli@ntnu.no (H. Li).

https://doi.org/10.1016/j.energy.2020.119582

Nomenclature

BTES	Borehole thermal energy storage
COP	Coefficient of performance
CT	Cooling tower
DH	District heating
DHW	Domestic hot water
DC	Data centre
HP	Heat pump
MS	Main substation
SH	Space heating
TES	Thermal energy storage
WT	Water tank

demand was reduced by 13% by recycling waste heat from a DC and two food stores [24]. However, there are some challenges hindering the utilization of waste heat from DCs for DH systems. One is the mismatch between DCs' waste heat supply and DH systems' heat demand [25]. The available waste heat from a DC depends on its load profile, which is usually spread equally. Therefore, the waste heat generated by DCs is at almost a constant rate [17,26]. In contrast, the heat demand in buildings is related to outdoor air temperature and occupant behaviour, which is full of fluctuations and uncertainties [27]. The resulting heat demand varies with the season, and even changes within one day. The difference between waste heat generation and heat demand leads to a mismatch between heat supply and heat demand. The mismatch problem would reduce the waste heat utilization rate and limit the economic and environmental benefits of utilizing DCs' waste heat [18].

One way to solve the mismatch in a DH system is to introduce thermal energy storage (TES). In a review by Shah et al., borehole thermal energy storage (BTES) was found to be an appropriate solution to solve the mismatch for solar DH systems in cold climates [28]. Rohde et al. studied an integrated heating and cooling system in Norway. BTES was proposed to solve the mismatch between heat supply (from solar collectors and the condensing heat) and heat demand [29,30]. Köfinger et al. studied a DH system with industrial waste heat recovery in Austria. Pit thermal energy storage was used to shift industrial waste heat from summer to autumn or winter, and supplied heat during peak hours [31]. Similarly, Moser et al. explored the use of large-scale (seasonal) heat storage to shift industrial waste heat from summer to winter and thereby made the feed-in of waste heat economically more attractive [32]. Tian et al. studied a hybrid solar DH system with both TES and back up boilers in Denmark. A water tank (WT) was applied as a short-term TES to relieve the mismatch between the heat supply from a solar heating plant and the heat demand in buildings [6].

Finally, peak load is an important issue in DH systems. Higher peak load will increase the initial investment and operation cost of a DH system. A survey shows that 87% of the current heating price models in Sweden take into account heat users' peak load [33]. These price models divide the heating bill into two parts: fixed and variable [34–37]. The fixed part is charged based on the peak load, and it accounts for 10–50% of the total heating bill [33]. Therefore, shaving the peak load will bring significant economic benefits for heat users.

Introducing TES is one way to shave the peak load in a DH system. Verda et al. studied the idea of using a WT to shave the peak load of a DH system in Italy. The WT was charged at night and shaved the peak load in the morning. The results showed that peak load shaving led to a reduction of 12% and 5% for the annual fuel use and fuel cost, respectively [38]. Harris investigated the DH systems in Sweden and found that almost all heating plants used WTs to shave the peak load. This measure reduced the installed capacity and improved the operation efficiency of heating plants [39]. Verrilli et al. proposed an optimal control strategy to reduce the operation and maintenance cost of a DH plant in Finland. The control strategy took advantage of the load shifting effect of WT and saved the cost by 8% [40]. Jebamalai et al. investigated the benefits of placing WTs in a DH system to decrease its peak load. The results showed that the centralized WT could reduce the total network investment cost by 4%, the substation level WT could reduce the costs by 5%, and the building level WT could reduce the costs up to 7% [41].

In summary, introducing TES is an effective way for mismatch relieving and peak load shaving in DH systems. However, to the best of the author's knowledge, there is limited research considering the two performance indicators of TES at the same time, especially for the DH systems with heat supply from DCs. Further research is needed to evaluate the system performance in terms of energy, economic, and environmental indicators after introducing TESs. Therefore, this study aimed to solve the mismatch problem and shave the peak load for the DH systems, where DCs supply waste heat, by introducing TESs. Different scenarios with the short-term or long-term TESs were proposed. Energy, economic, and environmental indicators were introduced to evaluate the system performance. The novelty of this study is summarized as followed: 1) This research focused on improving the utilization of DCs' waste heat in DH systems by introducing TESs, which is rarely addressed by existing studies. 2) Considering pricing schemes of DH, joint management of mismatch relieving and peak load shaving of TESs were investigated to optimize the economic performance. 3) For completeness of performance evaluation, research into both short-term and long-term TESs was conducted from aspects of energy efficiency, economic profits, and environmental impacts. 4) Sensitivity study of thermal storage efficiency was conducted to draw generalized conclusions on utilizing various TESs for waste heat supply from DCs.

The remainder of this article is organised as follows. Section 2 introduces the case study as the background for the system model. Section 3 presents the analysed scenarios, modelling approach, and methods used for economic and environmental analysis. Section 4 shows the model validation and simulation results. Section 5 presents the sensitivity analysis to investigate the impacts of TES storage efficiency. Finally, in Section 6, conclusions are presented.

2. Description of the case study

A campus DH system in Norway was chosen as the case study. The topology of the system is presented in Fig. 1. The system supplies heat to a total building area of 300,000 m^2, and the main functions of these buildings are education, offices, laboratories, and sports [42,43]. The campus DH system is connected to the city DH system by the main substation (MS). Apart from the heat supply from the city DH system, part of the annual heat supply comes from waste heat recovered from the university's DC. The current campus DH system faces two problems: 1) the mismatch between the heat supply from DC and the heat demand in buildings; 2) the higher peak load, which results in a large amount of money paid for it.

Fig. 2 shows the hourly mismatch between building heat demand and DC waste heat supply. During the non-heating season, the building heat demand came only from the domestic hot water (DHW) system. The heat demand ranged from 0.2 to 3.1 MW, which depended on occupant behaviour. During the heating season, the building heat demand came from both DHW needs and space heating (SH) system, which was negatively correlated with the

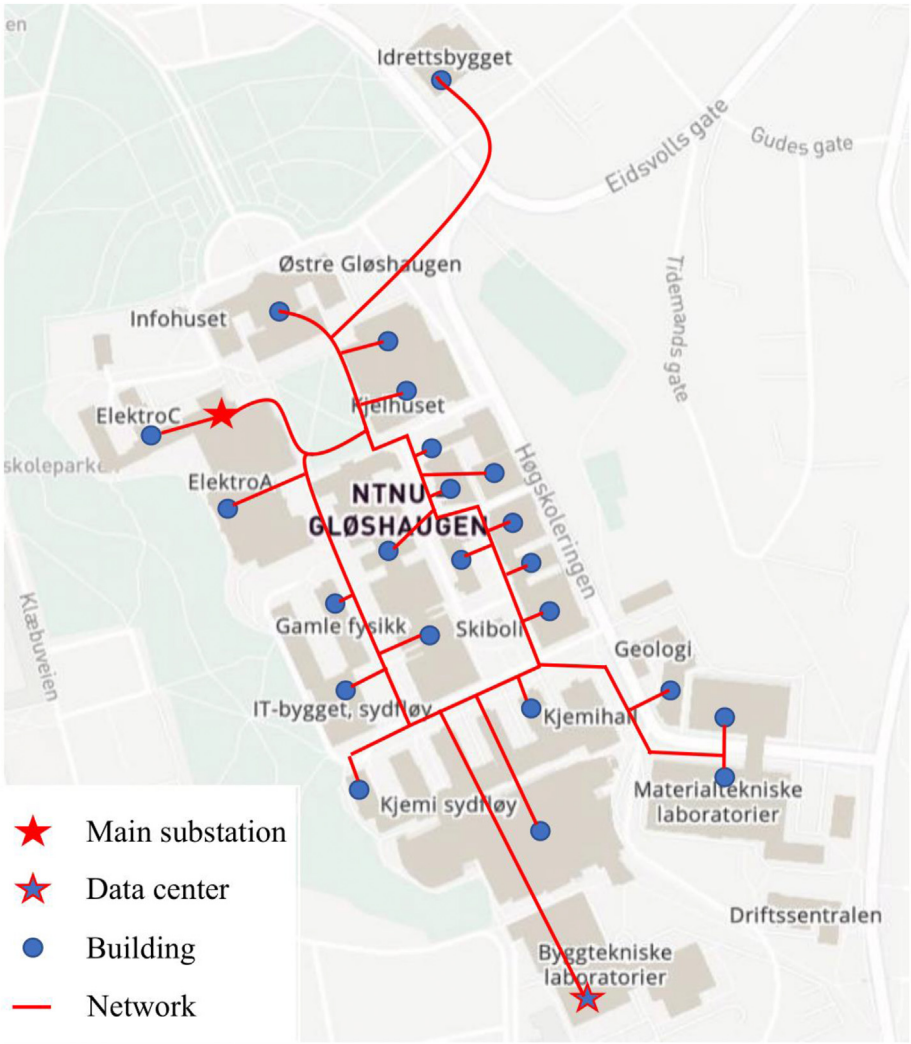

Fig. 1. Campus district heating system.

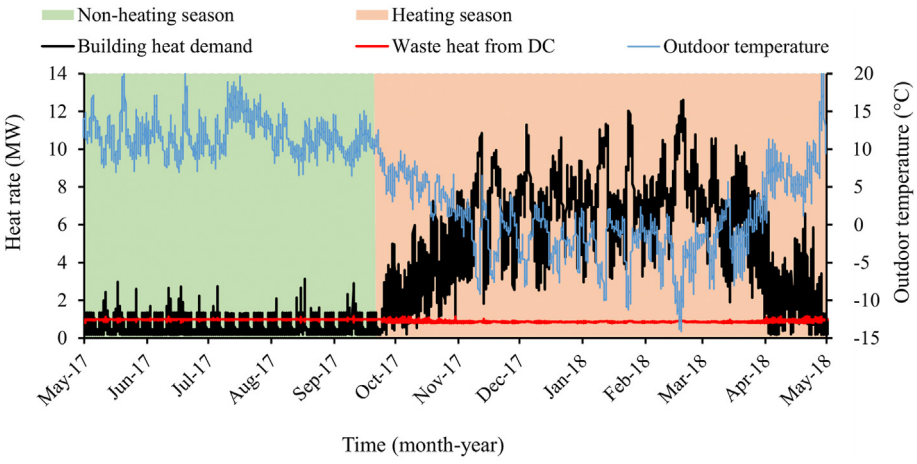

Fig. 2. Hourly building heat demand and data centre waste heat supply for the year 2017–2018.

outdoor temperatures. The heat demand ranged from 0.2 to 12.6 MW. In contrast, the DC waste heat supply was stable throughout the year, around 0.9 MW, see the red line in Fig. 2.

Fig. 3 illustrates the seasonal mismatch between building heat demand and DC waste heat supply. During the non-heating season, the supplied waste heat exceeded the heat demand. The total DC waste heat supply was 3.4 GWh, which was 1.4 GWh higher than the building heat demand, as shown in Fig. 3 at the left hand side.

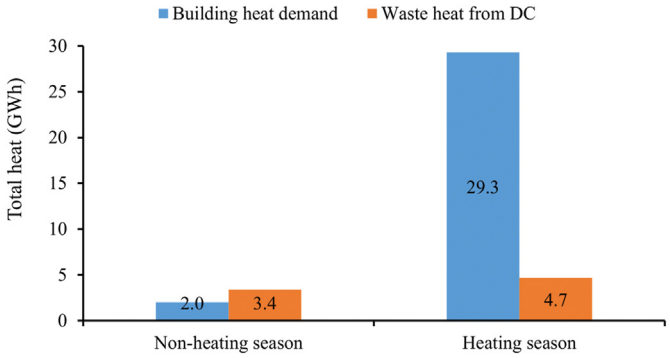

Fig. 3. Total building heat demand and data centre waste heat supply for the year 2017–2018.

During the heating season, the DC waste heat supply was far from satisfying the building heat demand. The waste heat supply was 4.7 GWh, while the building heat demand was 29.3 GWh, as shown in Fig. 3 at the right hand side.

In addition, as shown in Fig. 2, the building heat demand was not equally distributed and there were peak loads for both the heating and non-heating seasons. The maximum building heat demand was 12.6 MW during the heating season, which was about two times higher than the average value of 5.5 MW. Similarly, the maximum building heat demand was 3.1 MW during the non-heating season, which was about five times higher than the average value of 0.6 MW. The local DH company charges for heating based on heat use and peak load. The university pays about 4.7 million NOK[1] for the peak load each year. The money paid for the peak load accounts for 23% of the total heating bill.

3. Method

Three TES configurations were proposed to solve the mismatch problem and shave the peak load for the DH system, where the waste heat from the DCs was available. In addition, a reference scenario presenting the current campus DH system, was used as the benchmark to evaluate the system performance of the three TES scenarios. In total, the four scenarios were simulated in the Dymola platform. Finally, their system performance was evaluated and compared in terms of energy, economic, and environmental indicators. Detailed information on the research scenarios, modelling approach, and economic and environmental analysis methods are introduced in this section.

3.1. Suggested scenarios to include TESs

Fig. 4 shows schematics of the four scenarios. The reference scenario, *Ref*, presented the current campus DH system, see Fig. 4 a). In this scenario, the city DH system acted as the basic heat source and supplied heat through the MS. Meanwhile, the DC functioned as an additional heat source. The condensing heat of the DC cooling system was fed into the return line of the campus DH ring. This scenario suffered from the mismatch and high peak load problems, as introduced in Section 2.

The scenario *Ref* + *WT* integrated a WT into the reference scenario *Ref*, see Fig. 4 b). The volume of the WT was chosen as 8,000 m^3, which was able to supply heat to the campus DH system for two days. The WT functioned as the short-term TES. It aimed to relieve the mismatch between the DC waste heat supply and the building heat demand during the non-heating season. The WT operated in charging mode when the DC waste heat supply was higher than the building heat demand, otherwise, it operated in discharging mode. During the heating season, the WT was used to shave the peak load. It operated in discharging mode during the peak load hours, otherwise, it operated in charging mode.

The scenario *Ref* + *BTES* integrated a BTES system, that included a heat pump (HP) and a borehole field, into the reference scenario *Ref*, see Fig. 4 c). The borehole field contained 240 single U-tube boreholes. The depth of the boreholes was 55 m, and the distance between each borehole was 3 m. All boreholes were connected in parallel. The borehole field was sized with a charging rate of 1.1 MW, which was 80% of the maximum heat rate of the waste heat supply [44]. During the non-heating season, the BTES system operated in charging mode, storing the surplus waste heat supplied by the DC. In charging mode, the HP was not in operation, and the BTES system and DC were connected in series. During the heating season, the BTES system switched to discharging mode. However, it operated only during the peak load hours. In discharging mode, the long-term TES system and the DC were connected in parallel, working together to supply heat to the campus DH system.

The scenario *Ref* + *WT* + *BTES* integrated both a WT and a BTES system into the reference scenario *Ref* , see Fig. 4 d). During the non-heating season, the WT was used to solve the hourly mismatch problem. In addition, the BTES system operated in charging mode to solve the seasonal mismatch problem. As presented in Fig. 3, about 1.4 GWh excess waste heat was supplied during the non-heating season. The BTES system was used to shift this part of waste heat to the heating season. During the heating season, the WT and BTES worked together to shave the peak load. The charging and discharging strategies were the same as in scenarios *Ref* + *WT* and *Ref* + *BTES*.

3.2. Modelling approach for the campus DH system

The Dymola model of the campus DH system is presented in Fig. E1 of Appendix E. The model has the following components: buildings, DC, WT, BTES, and MS. The approach used to model these components is explained in this section and the key parameter settings are presented in Table A.1, B.1, C.1, C.2, C.3 and D.1 of Appendices A-D.

3.2.1. Building model

A single-equivalent building model was used to represent the overall performance of all the buildings on campus. The properties of the equivalent building were determined by summing or weighting the average properties of individual buildings. For example, the area of the exterior wall of the equivalent building was calculated by summing the corresponding values for all the buildings, and the U-value of the exterior wall of the equivalent building equalled the weighted average value of the corresponding values of all the buildings. The equivalent building model enabled increased computational efficiency, while maintaining high simulation accuracy. As shown in Fig. 5, the building model contained six modules: building envelope, internal heat gain, SH system, DHW system, ventilation system, and weather.

The building envelope module was developed based on the *TwoElements* component of the *Buildings* library [45]. It used an RC thermal network to represent the thermal process. Detailed information about this component can be found in Ref. [46]. The internal heat gain module defined the heat rate of the internal heat gain from the building's equipment, lighting, and occupants. The ventilation system module represented the building's ventilation system and specified its airflow rate and heat recovery efficiency.

[1] The currency rate between NOK and EUR can be found from https://www.xe.com/, in this study 1 EUR = 9.5 NOK.

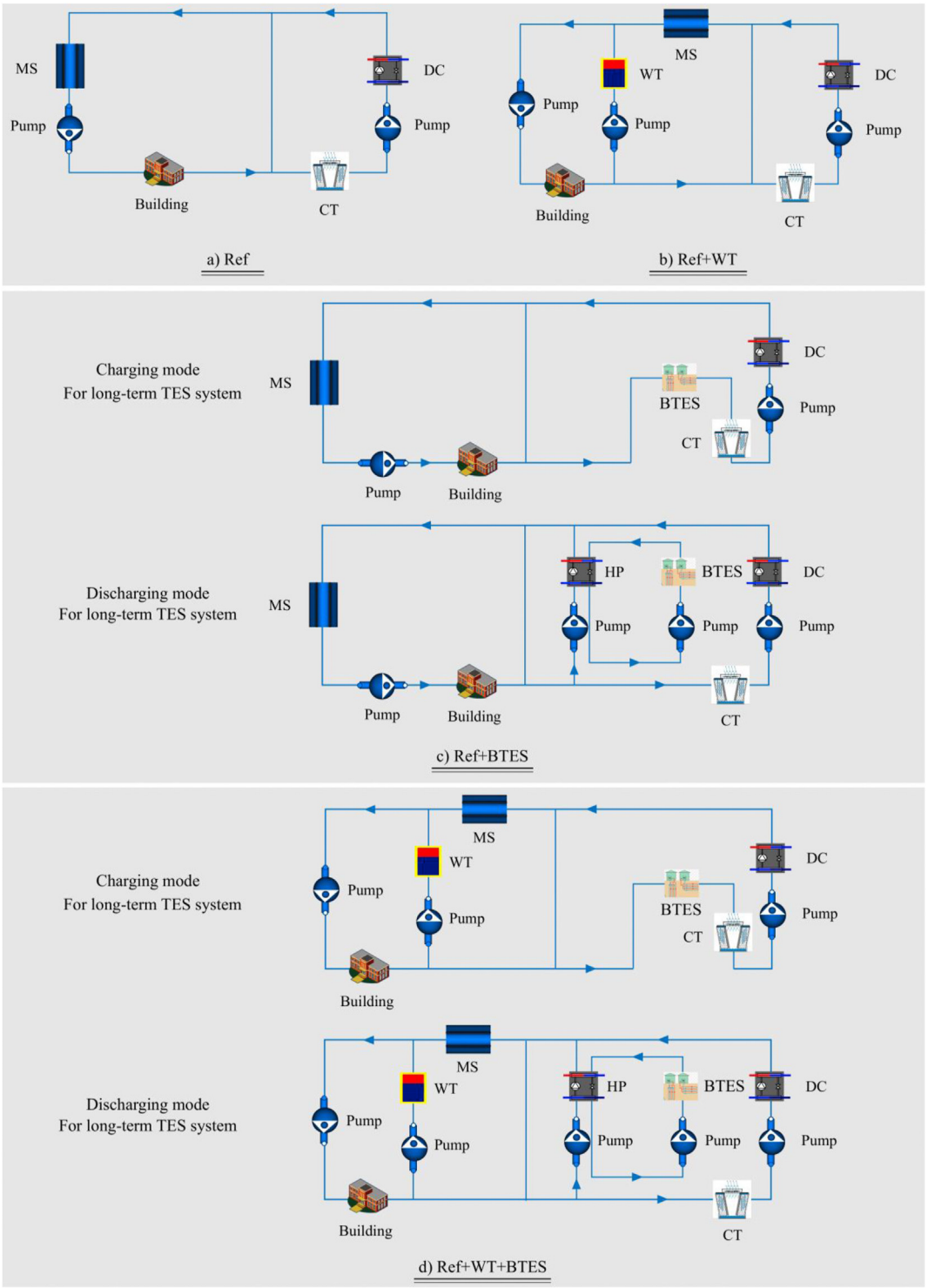

Fig. 4. Schematics of the four scenarios.

The SH and DHW system modules represented the SH and DHW systems of the buildings. The main components of these modules included radiator, pumps, heat exchangers, water taps, and pressurization systems. All these components came from the *Modelica Standard Library* [47] and libraries from IBPSA Project 1 [48].

3.2.2. Data centre model

The DC model is shown in Fig. 6. The key components were the HP and the cooling tower (CT). The HP connects the DC cooling system to the campus DH system. Its evaporator side produces chilled water for the cooling system, while its condenser side feeds waste heat into the campus DH system. The HP model was built based on the *Carnot_y* component in the *IDEAS* library [49]. This calculates the coefficient of performance (COP) based on the nominal COP, Carnot efficiency, and part-load efficiency. Detailed information on the *Carnot_y* component can be found in Ref. [50].

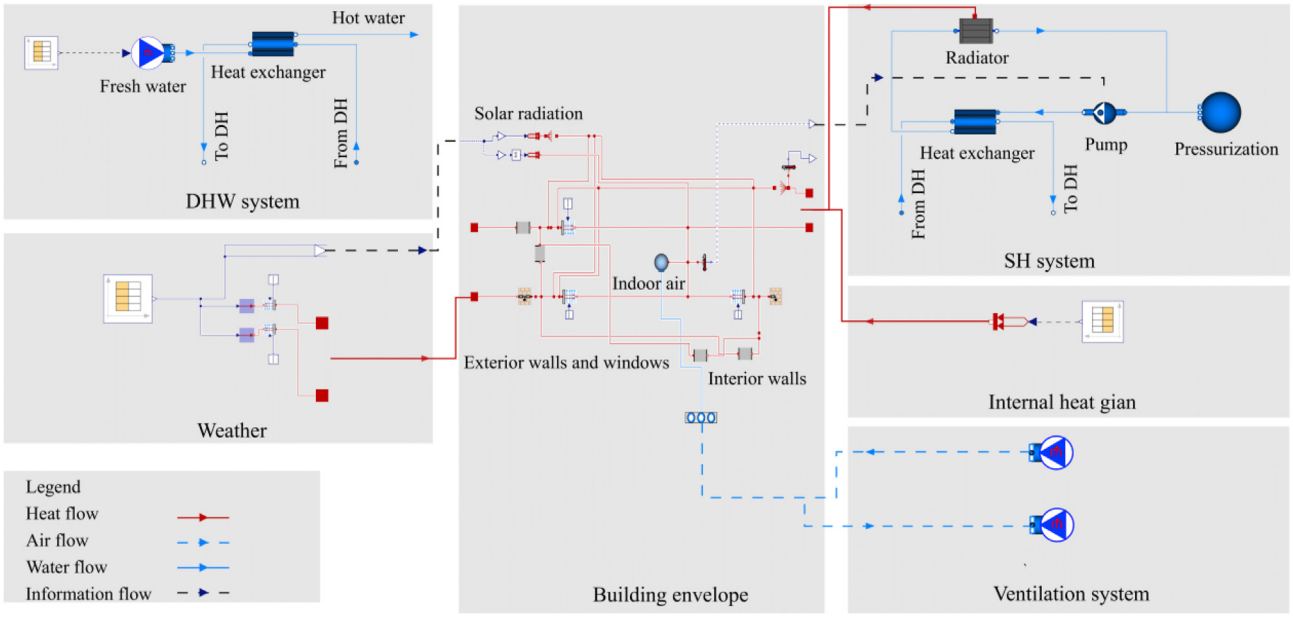

Fig. 5. Building model.

The CT is used to guarantee the safe operation of the DC cooling system. It starts to work when the incoming water temperature at the condenser side exceeds the safety level.

3.2.3. Water tank and borehole thermal energy storage system model

The WT model came from the *StratifiedEnhanced* component of the *AixLib* library [51]. The model used several sections to represent stratification, and the thermal process of each section was described by the laws of energy conservation. Detailed information about the model can be found in Ref. [52].

The BTES system model is shown in Fig. 7. Its key components were BTES and HP. The BTES model was developed based on the *OneUTube* component of the *IDEAS* library. The model calculated the thermal processes using an axial discretized resistance-capacitance network. Detailed information on the BTES model can be found in Ref. [53].

3.2.4. Main substation model

The MS connects the city DH system to the campus DH system. The MS has two functions. First, it supplements the heat supply when waste heat cannot cover the heat demand. Second, it further boosts the supply temperature when the supply temperature from the DC is insufficient for the building system. As shown in Fig. 8, the key component of the MS model was the heat exchanger. The heat exchanger model was based on the *BasicHX* component of the *Modelica Standard Library* [54].

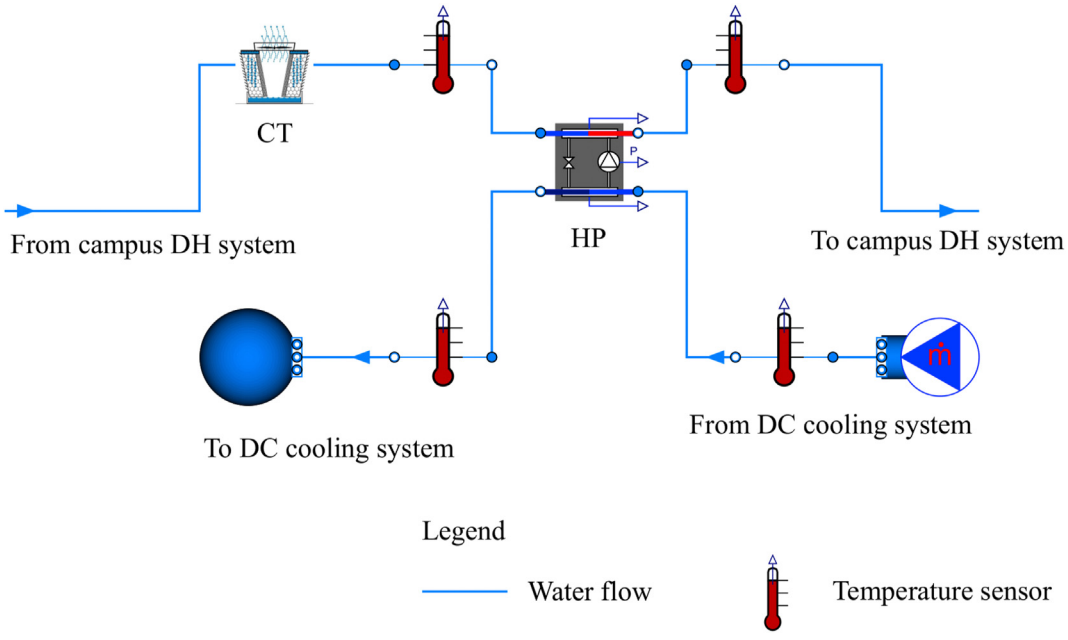

Fig. 6. Data centre model.

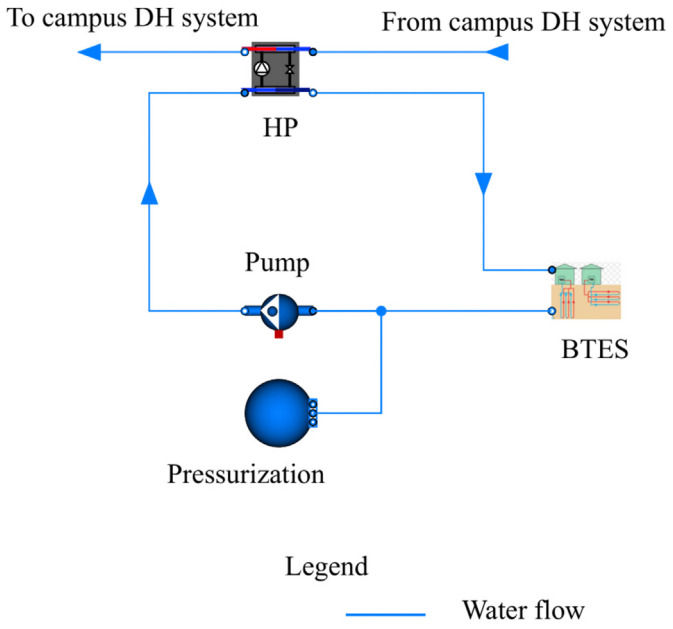

Fig. 7. Borehole thermal energy storage system model.

3.3. Method for economic analysis

3.3.1. Initial investment for a TES system

The initial investment required for a TES system varies with the storage type and depends strongly on the storage size. Fig. 9 illustrates the relationship between initial investment and size for a WT and a BTES system. The solid black dots in Fig. 9 represent previous projects [55]. The figure shows that power functions approximate the relationship very well, with coefficients of determination (R^2) higher than 0.8 and no obvious overfitting. In this study, the power functions were used to estimate the initial investment for the TES system. For the BTES system, initial investment in the HP was also considered. The unit cost of the HP was assumed to be 0.8 million EUR/MW, based on a report that studied large scale HPs for DH systems [56].

3.3.2. Calculation of energy bill

The energy bill includes the heating and electricity bills, which are explained as follows.

The heating bill contains two parts: fixed and variable, as presented in Eq. (1).

$$B_{heat(tot)} = B_{heat(fix)} + B_{heat(\mathrm{var})} \tag{1}$$

where $B_{heat(tot)}$ is the total heating cost, $B_{heat(fix)}$ is the fixed part, and $B_{heat(var)}$ is the variable part.

The fixed part is calculated in Eq. (2) as follows:

$$B_{heat(fix)} = \dot{Q}_{peak,sum} P_{heat(fix,sum)} + \dot{Q}_{peak,win} P_{heat(fix,win)} \tag{2}$$

where $\dot{Q}_{peak,sum}$ and $\dot{Q}_{peak,win}$ are the peak load for the summer and winter seasons, respectively. $P_{hit(fix,sum)}$ and $P_{heat(fix,win)}$ are the unit fixed heating price for the summer and winter seasons, respectively.

The variable part is calculated in Eq. (3) as:

$$B_{heat(\mathrm{var})} = Q_{heat} P_{heat(\mathrm{var})} \tag{3}$$

where Q_{heat} is the total heat use, and $P_{heat(var)}$ is the variable heating price. The unit fixed and variable heating price was obtained from the local DH company, Statkraft Varme, in Trondheim [57,58].

The electricity bill includes also a fixed part and a variable part. However, the fixed part in Norway is determined by the electricity use. However, a simplified electricity bill calculation method was proposed in Eq. (4). This method assumed that the electricity bill contained only the variable part, and it was a function of electricity use. The equivalent electricity price was calculated as:

$$B_{elec} = E_{elec} P_{elec} \tag{4}$$

where B_{elec} is the electricity cost, E_{elec} is the electricity use, and P_{elec} is the equivalent electricity price. The equivalent electricity price is equal to the total electricity cost (including the fixed and variable parts) divided by the electricity use. In this study, the equivalent electricity price was 1.07 NOK/kWh.

3.3.3. Calculation of the payback period

The payback period is the time taken to fully recover the initial investment. It is one of the most commonly used methods for evaluating initial investments [59]. The payback period *PB* is calculated using Eq. (5):

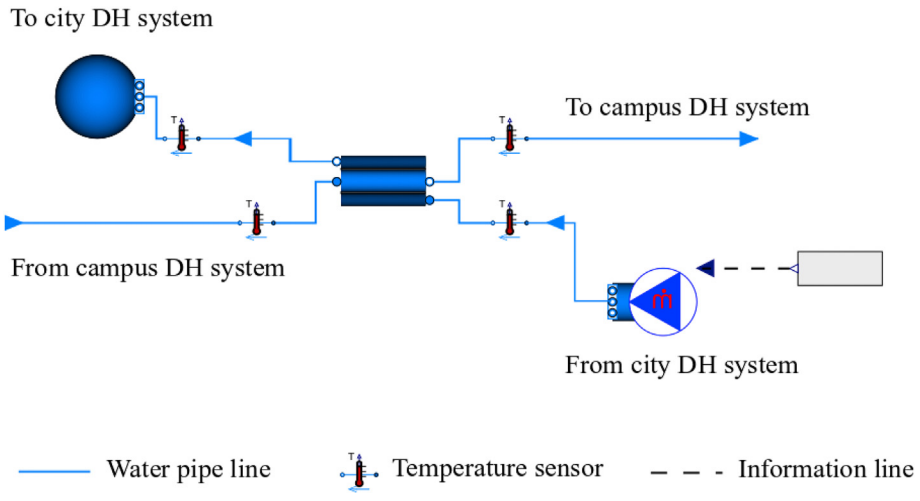

Fig. 8. Main substation model.

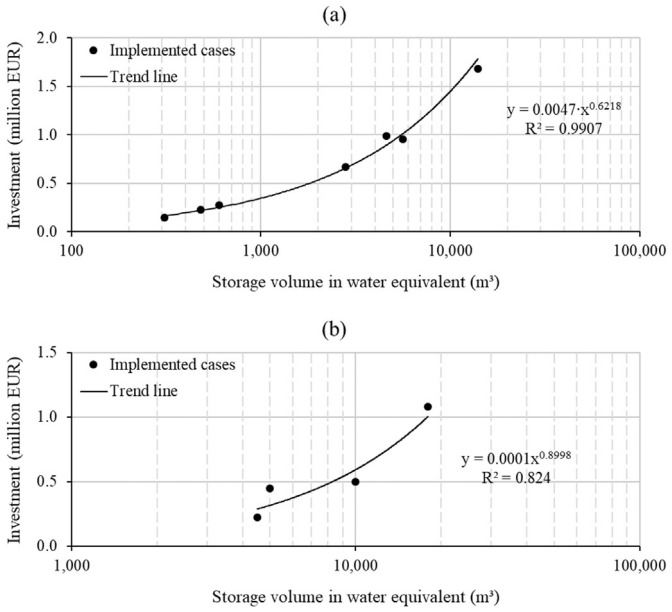

Fig. 9. Investment in thermal energy storage with different sizes, (a) water tank and (b) borehole thermal energy storage.

$$B_{sav}\frac{(1+i)^{PB}-1}{i(1+i)^{PB}}-Invt=0 \tag{5}$$

where B_{sav} is the annual energy bill saving. $Invt$ is the initial investment. i is the prevailing interest rate, for which 2% was used in this study [60].

3.4. Method for environmental analysis

The increase in global average temperatures is attributed to an increase in greenhouse gas emissions, especially CO_2 [61]. Therefore, this study used CO_2 emissions as an indicator to evaluate environmental impact.

As shown in Eq. (6), a CO_2 emission factor is used to calculate CO_2 emissions as:

$$EM_{CO2}=E\times EF \tag{6}$$

where EM_{CO2} is the CO_2 emission, E is heat or electricity use, and EF is the CO_2 emission factor for heat or electricity.

The reference value for the CO_2 emission factor for heat was obtained from the local DH company as 51.8 g/kWh [57]. This value considers the entire life-cycle emissions of all types of fuel, including waste incineration, biomass, liquefied petroleum gas, etc. The reference value for the CO_2 emission factor for electricity was 18.9 g/kWh [62]. This low value is attributed to the high proportion of renewable electricity in Norway. About 98% of electricity is from hydropower and wind power.

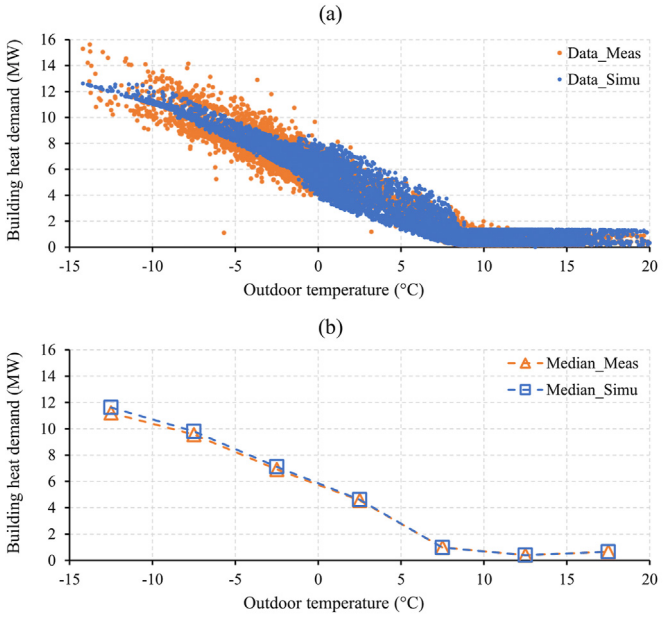

Fig. 10. Simulated and measured hourly building heat demand plotted against outdoor temperature, (a) original simulated and measured data, and (b) medians with an interval of 5 °C and their trend lines.

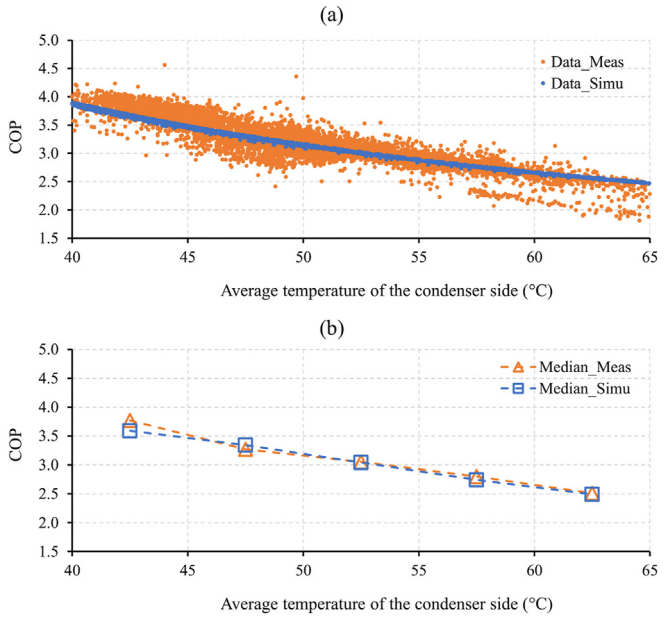

Fig. 11. Simulated and measured COP plotted against the average water temperature of the condenser side, (a) original simulated and measured data, and (b) medians with an interval of 5 °C and their trend lines.

4. Results

This section first presents the model validation, then evaluates

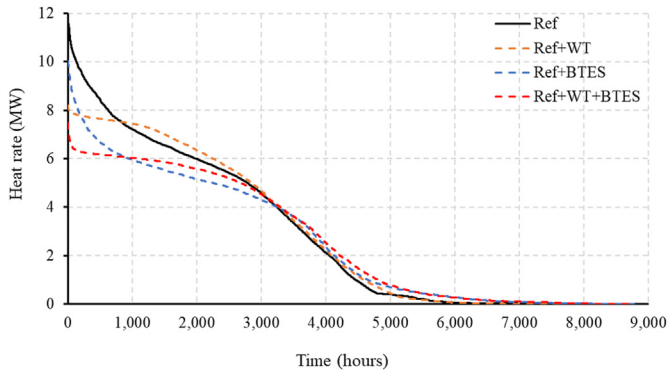

Fig. 12. Heat load duration diagram for the four scenarios.

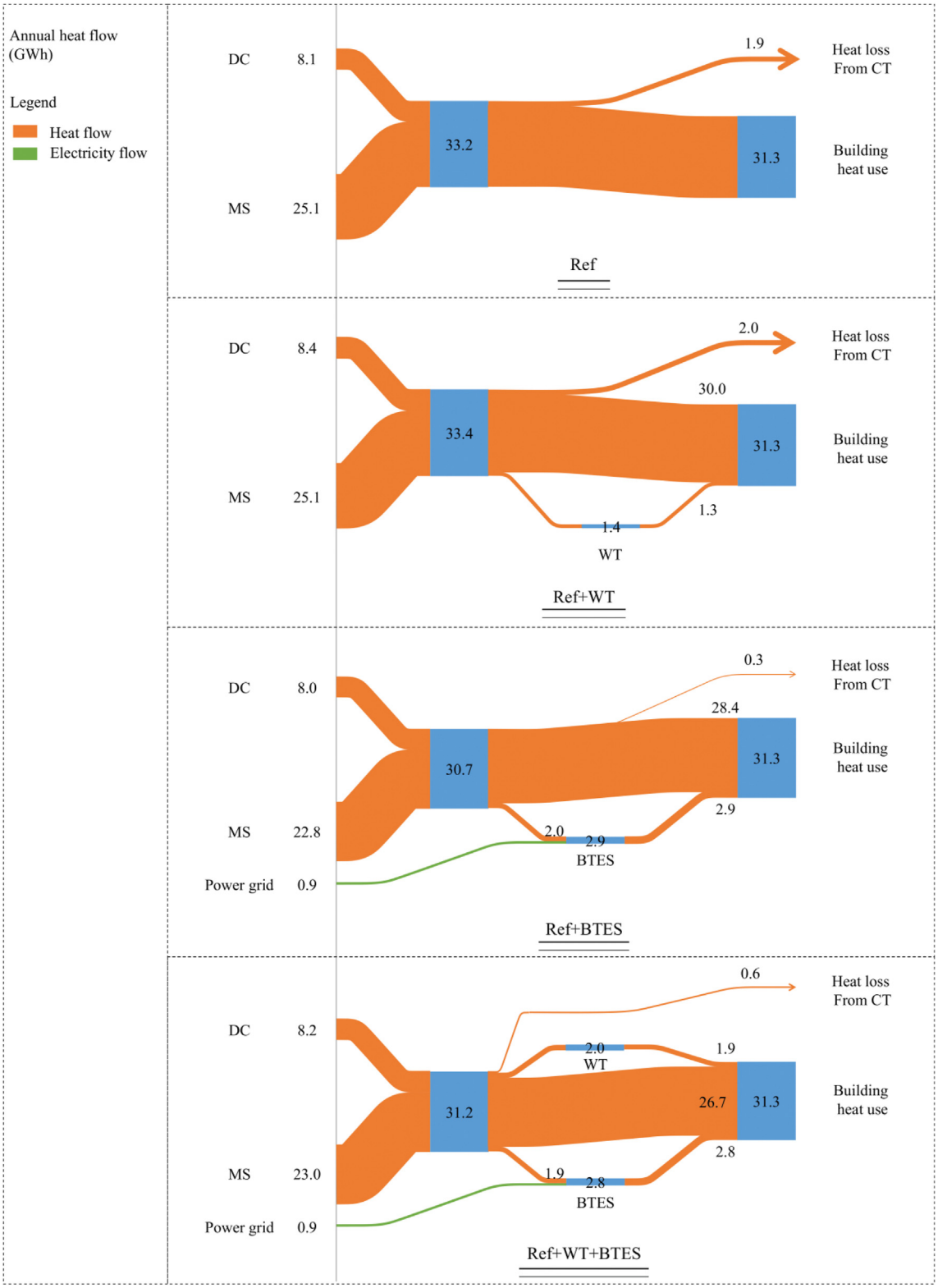

Fig. 13. Annual heat flow for the four scenarios.

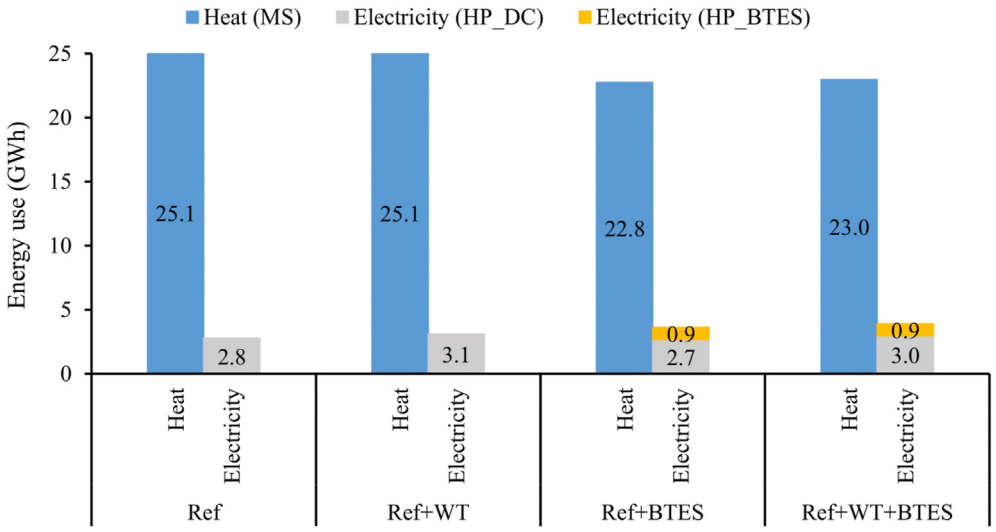

Fig. 14. Annual heat supply and electricity use for the four scenarios.

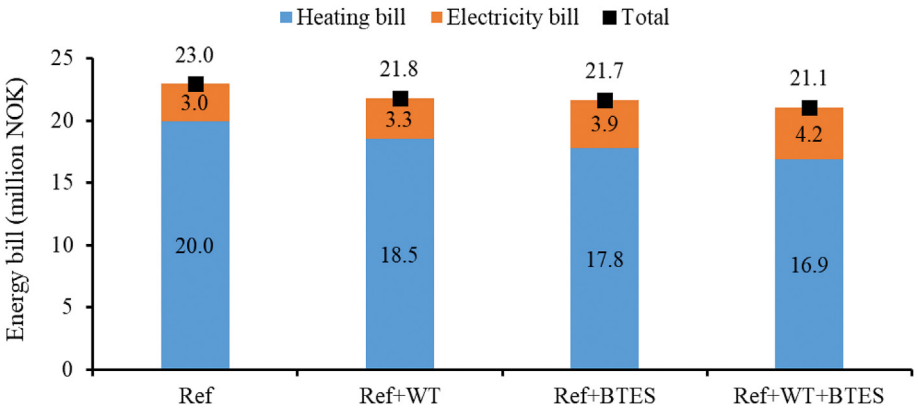

Fig. 15. Annual heat and electricity bills for the four scenarios.

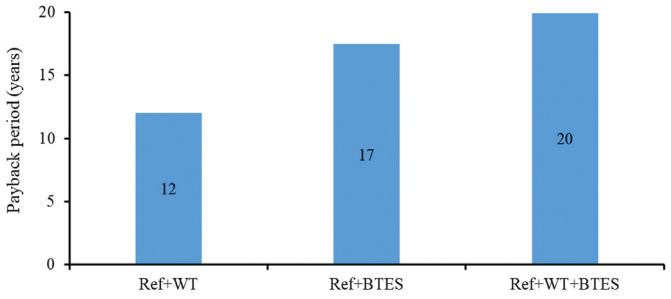

Fig. 16. Payback period for the three TES scenarios.

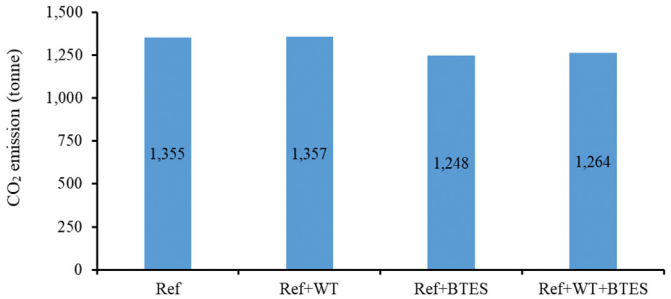

Fig. 17. Annual CO_2 emissions for the four scenarios.

the three TES scenarios based on energy, economic, and environmental analyses.

4.1. Model validation

The building and HP models were validated by the measured data from the campus energy management platform. The validation of the building model is presented in Fig. 10. The simulated and measured hourly building heat demands exhibited a similar pattern. During the heating season, the building heat demand was negatively correlated with the outdoor temperature. However, this correlation disappeared during the non-heating season. In addition, the median of the simulated building heat demand matched the measured value at the same interval. The errors of these medians were within ±4%. Similarly, the simulated total building heat demand also matched the measured data, which were 31.3 GWh and 31.4 GWh, respectively. The error in the total building heat demand was within ±1%.

For a typical water source HP, the COP is a function of condensation and evaporation temperatures. These cannot be measured

Table 1
Scenarios of sensitivity analysis.

Name	WT efficiency (%)	BTES efficiency (%)
Ref + WT	100	–
Ref + WT9	90	–
Ref + WT8	80	–
Ref + WT7	70	–
Ref + WT6	60	–
Ref + WT5	50	–
Ref + BTES	–	100
Ref + BTES9	–	90
Ref + BTES8	–	80
Ref + BTES7	–	70
Ref + BTES6	–	60
Ref + BTES5	–	50

directly, but the water temperatures on the condenser and evaporator sides can be used instead. In this study, the influence of the evaporation temperature was ignored because the water temperature on the evaporator side remained approximately constant (with inlet and outlet temperatures of 11 and 7 °C, respectively). Therefore, the relationship between the COP and the water temperature at the condenser side was used to validate the HP model. Fig. 11 presents the validation of the HP model. Please note that the average water temperature at the condenser side refers to the average value of the inlet and outlet water temperatures. The simulated COP agreed very well with the measured COP. They exhibited the same trend, with the COP decreasing when the water temperature increased at the condenser side. Meanwhile, the median of the simulated and measured COP was calculated at the same interval. The errors of those medians were within ± 5%.

4.2. Evaluating the TES scenarios by energy analysis

This section evaluates the TES scenarios based on energy analysis. Fig. 12 illustrates the heat load duration curves of the campus DH system, which was used to evaluate the peak load shaving effect. Fig. 13 and Fig. 14 show the heat balance and energy use, which were used to evaluate the mismatch reliving effect. Please note that the heat load refers to the heat rate of heat supply from the MS. The heat loss refers to the amount of heat removed by the CT as a result of the mismatch problem. During the non-heating season, more waste heat was supplied than the building heat demand, and this surplus waste heat would ultimately become heat loss. In addition, the additional pumping electricity use for TESs was not accounted for in this study, because it was negligible compared to the HP electricity use. For a typical DH system, the demand for electricity for pumping is only about 0.5% of the heat delivery [1].

As shown in Fig. 12, the WT contributed to a significant peak load shaving effect. The peak load of the scenario *Ref* + *WT* dropped to around 8.1 MW, a reduction of almost 30% compared to the reference scenario *Ref*. However, introducing the *WT* did not relieve the mismatch problem and consequently did not reduce the MS heat supply. As shown in Figs. 13 and 14, the scenario *Ref* + *WT* even showed a slightly higher heat loss than the reference scenario *Ref*. This was because the DC waste heat supply increased with the introduction of the *WT*. During the *WT* charging process, the outlet water from the *WT* and the return water from the building mixed together, and then became the inlet water for the HP of the DC. The outlet temperature from the *WT* was usually higher than the return temperature from the building, so the *WT* charging process increased the inlet temperature of the HP. This increased temperature led to a higher condensation temperature and a lower COP for the HP. Therefore, more waste heat was generated to produce the same amount of cooling.

However, the BTES system almost solved the mismatch problem and saved a considerable amount of MS heat supply. As shown in Fig. 13, the scenario *Ref* + *BTES* reduced the heat loss by 83% compared to the reference scenario *Ref*. The surplus waste heat was stored by the BTES system during the non-heating season and then supplied to the building during the heating season. This long-term heat storage shifted the waste heat from non-heating season to heating season, and thus increased the waste heat utilization rate from 77% to 96%. Consequently, as shown in Fig. 14, the annual heat supply from MS was reduced by 10%. In addition, the BTES system also brought a remarkable peak load shaving effect, although this was less significant than in the case of the WT. As shown in Fig. 12, the peak load of the scenario *Ref* + *BTES* was 15% lower than the reference scenario *Ref*.

The scenario *Ref* + *WT* + *BTES*, which combined a WT and a BTES system, had the most complex system, as shown in Fig. 4. The peak load shaving effect achieved the best performance due to the combination of WT and BTES, a reduction of 37%, as illustrated in Fig. 12. However, the mismatch relieving effect was worse than the scenario *Ref* + *BTES*. The heat loss and the MS heat supply were reduced by 68% and 9%, respectively, as presented in Fig. 14.

In addition, both the *WT* and *BTES* scenarios used more electricity than the reference scenario. As shown in Fig. 14, the scenario *Ref* + *WT* increased electricity use by 12%. This was because the WT charging process led to a higher condensation temperature for the HP in the DC, and thus increased HP electricity use, as explained above. Similarly, the *Ref* + *BTES* scenario increased electricity use by 30%. This was caused by the additional electricity use of the HP in the BTES system, which was 0.9 GWh per year. The scenario *Ref* + *WT* + *BTES* resulted in the largest increase in electricity use, amounting to 40%. This was because it not only increased electricity use from the HP in the DC but also resulted in additional electricity use by the HP in the BTES system.

4.3. Evaluating the TES scenarios by economic analysis

This section evaluates the TES scenarios based on economic analysis. As shown in Fig. 15, both the WT and the BTES system could save energy bills. The scenario *Ref* + *WT* saved 5% of the annual energy bill compared to the reference scenario *Ref*. This saving arose only due to the reduction in the fixed part of the heating bill, which was brought by the peak load shaving effect of the WT. Similarly, the scenario *Ref* + *BTES* saved 6% of the annual energy bill. This bill saving came from the reduction in both the fixed and variable parts of the heating bill, which was caused by the peak load shaving and mismatch reliving effects of the BTES. In addition, the scenario *Ref* + *WT* + BTES achieved the highest energy bill saving, reducing the bill by 8%. This was because it made full use of the advantages of both the WT and BTES.

Fig. 16 presents the payback period of the three TES scenarios. The scenario *Ref* + *WT* had the shortest payback period of 12 years. In contrast, the *Ref* + *BTES* and *Ref* + *WT* + *BTES* scenarios presented longer payback periods of 17 and 20 years, respectively, although they had better annual energy bill savings. These long payback periods were due to the high initial investment.

4.4. Evaluating the TES scenarios by environmental analysis

This section evaluates the TES scenarios based on environmental analysis. As shown in Fig. 17, the BTES system effectively reduced CO_2 emissions. The *Ref* + *BTES* and *Ref* + *WT* + *BTES* scenarios reduced the annual CO_2 emissions by 8% and 7%, respectively. This significant reduction was for two reasons. First, the BTES system almost solved the mismatch problem and consequently saved a considerable amount of MS heat supply. Second, the CO_2 emission

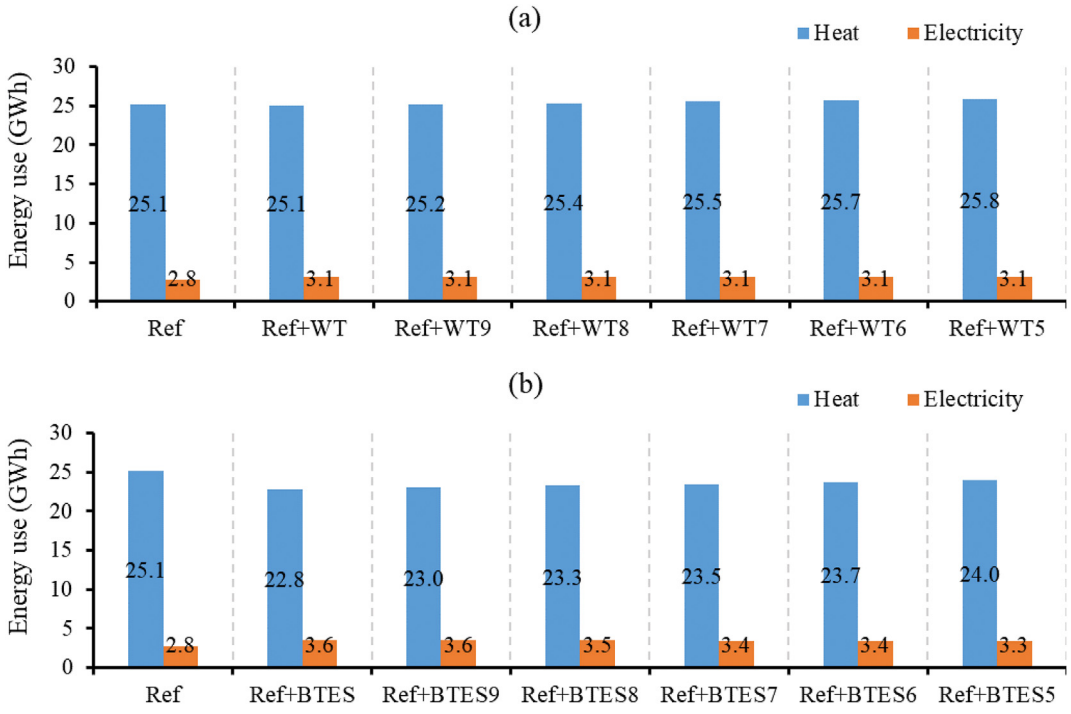

Fig. 18. Annual energy use for the water tank scenarios (a) and the borehole thermal energy storage scenarios (b).

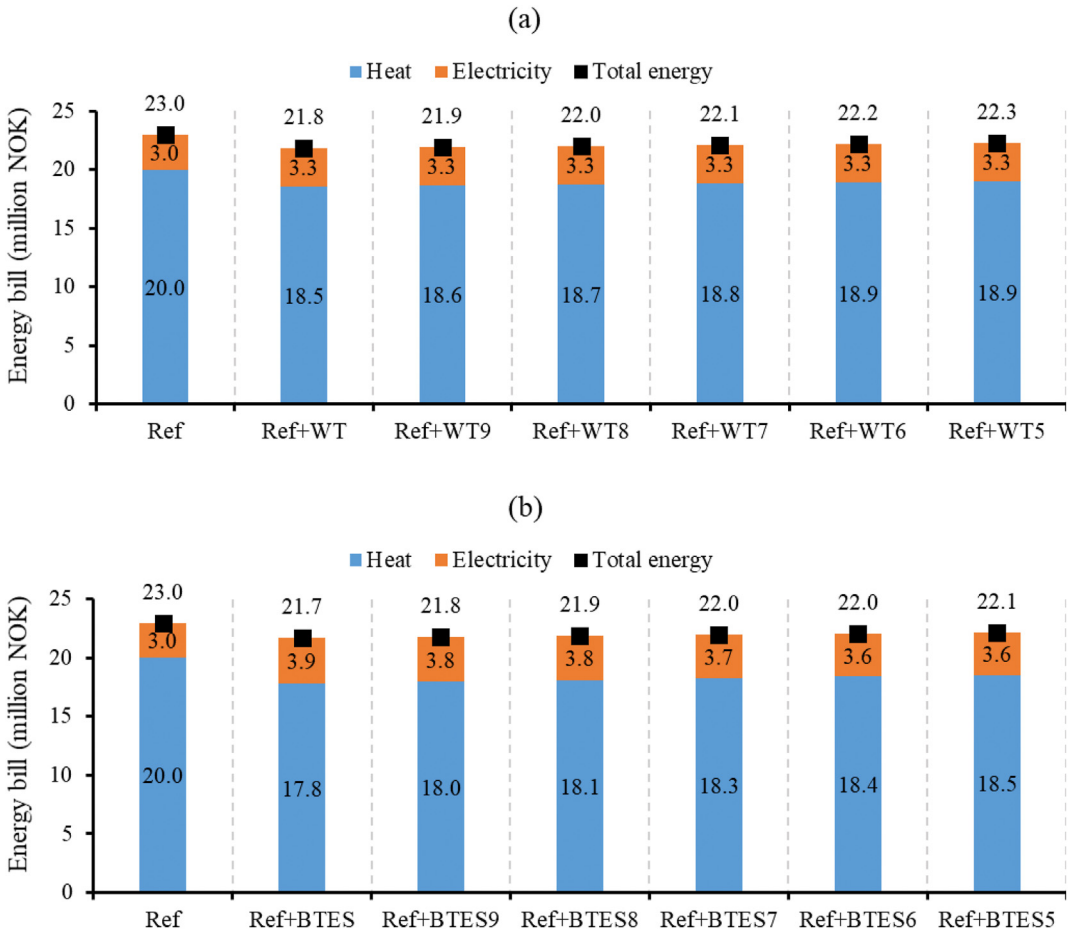

Fig. 19. Annual energy bill for the water tank scenarios (a) and the borehole thermal energy storage scenarios (b).

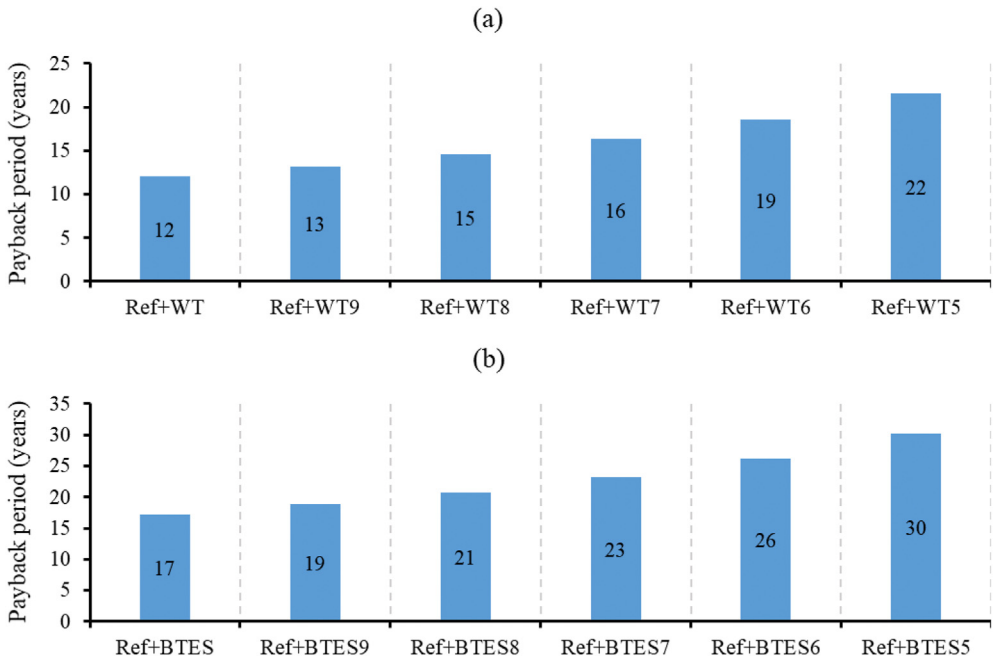

Fig. 20. Payback period for the water tank scenarios (a) and the borehole thermal energy storage scenarios (b).

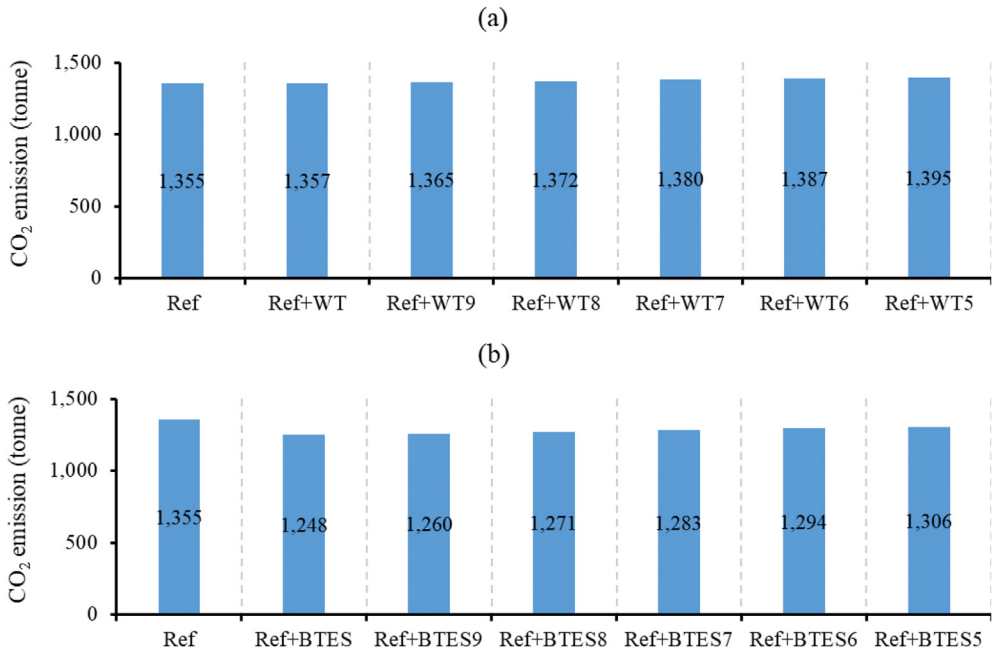

Fig. 21. Annual CO_2 emission for the water tank scenarios (a) and the borehole thermal energy storage scenarios (b).

factor for electricity was much smaller than that for heat, even though electricity use increased with the introduction of BTES. Therefore, the decrease in the CO_2 emissions from heat was much larger than the increase in CO_2 emissions from electricity. In contrast, the WT did not bring any benefits in terms of reducing CO_2 emissions, because it had no obvious heat-saving effect.

5. Sensitivity analysis of thermal energy storage efficiency

The results from Section 4 assumed that the TES has a storage efficiency of 100%. However, the storage efficiency ranges from 50% to 100% for the WT and BTES, based on a report from the International Energy Agency on large scale TESs [55]. The storage efficiency

of TESs differs from case to case and even changes with time. For example, the storage efficiency of BTES is highly related to its local geological condition. The storage efficiency of WT may reduce after several years' operation due to the moistened insulation. Therefore, it is necessary to conduct a sensitivity study to investigate the impacts of storage efficiency on different TESs, and thus provide more generalized suggestions on choosing different TESs. This section conducts a sensitivity analysis of storage efficiency. The study was conducted based on the principle of energy balance, which meant that heat loss from the TES would be supplemented by the MS. The annual MS heat supply and electricity use for the *Ref* + *WT* and *Ref* + *BTES* scenarios was used as the benchmark, which is presented in Fig. 14.

Table 1 presents the scenarios used for sensitivity analysis. The sensitivity analysis did not include the scenario with both the WT and BTES. The scenario *Ref* + *WT* + *BTES* did not achieve the best performance in terms of energy saving and CO_2 emissions reduction, even though it had the most complex system and the highest initial investment.

Fig. 18 shows the variation in the annual energy use as the storage efficiency of the TES varies. The MS heat supply increased with the decreased storage efficiency of the WT and BTES. In the WT scenarios, the annual MS heat supply would increase by 0.6% if the storage efficiency decreased by 10%. When the storage efficiency declined to less than 90%, the WT scenarios would require more MS heat supply than the reference scenario. In the BTES scenarios, the annual MS heat supply increased by 1.1% when the storage efficiency decreased by 10%. However, the BTES scenarios still had 5% less MS heat supply than the reference scenario, even when the storage efficiency dropped to 50%. In addition, the lower storage efficiency could reduce the electricity use for the BTES scenarios, because less stored heat was recovered by the HP of the BTES system.

Fig. 19 presents the variation in the annual energy bill as the storage efficiency of the TES varies. The annual energy bill would increase by 0.4% when the storage efficiency of the WT and BTES declined by 10%. However, the annual energy bills were still saved by 3–4%, even when the storage efficiency of the WT and BTES dropped to 50%. The increased annual energy bill led to a longer payback period for both the WT and BTES scenarios. As illustrated in Fig. 20, the payback period would increase by 2–4 years when the storage efficiency of the WT and BTES decreased by 10%. The WT scenarios would have a reasonable payback period of fewer than 15 years, if the storage efficiency remained higher than 80%. In contrast, the BTES scenarios presented a longer payback period of more than 17 years. The payback period could even be up to 30 years if the storage efficiency dropped to 50%.

Fig. 21 presents the variation in the annual CO_2 emissions as the storage efficiency of the TES varies. The lower storage efficiency increased the CO_2 emissions in both the WT and BTES scenarios. When the storage efficiency decreased by 10%, the increase was about 0.5% for the WT scenarios and 0.9% for the BTES scenarios. However, the BTES scenarios could always maintain lower CO_2 emissions compared to the reference scenario. The reduction of CO_2 emissions was around 4%, even when the storage efficiency dropped to 50%.

6. Conclusion

Three TES scenarios were proposed to address the mismatch problem and shave the peak load for the DH system, where the waste heat from data centre was available. The system performance was evaluated in terms of energy, economic, and environmental indicators. A campus DH system in Norway was selected as the case study.

The WT scenario was able to shave the peak load by up to 31%, which saved the annual energy bill by 5%. Meanwhile, the payback period was fewer than 15 years when the storage efficiency remained higher than 80%. However, introducing the WT had no obvious benefits in terms of mismatch relieving and CO_2 emissions reduction.

In contrast, the BTES scenario was able to improve the system performance substantially in terms of mismatch reliving and CO_2 emissions reduction. The waste heat utilization rate was increased from 77% to 96%, and the CO_2 emissions was reduced by up to 8%. In addition, the BTES also shaved the peak load by 15%, although this was less remarkable than the reduction achieved by the WT. Consequently, the annual energy bill was saved by 6% due to the mismatch reliving and peak load shaving. However, the BTES scenario presented a longer payback period of more than 17 years.

The scenario with both the WT and the BTES, had the most complex system and the highest initial investment. However, the system did not achieve the best performance in terms of energy saving and CO_2 emissions reduction. In addition, it had the longest payback period of 19 years, even without considering any heat loss.

These results provide guidelines for the retrofit of district heating systems, where data centres' waste heat is available.

Credit author statement

Haoran Li, Conceptualization, Methodology, Software, Validation, Writing – original draft. Juan Hou, Conceptualization, Software, Writing – original draft. Tianzhen Hong, Conceptualization, Writing – review & editing. Yuemin Ding, Conceptualization, Writing – review & editing. Natasa Nord, Conceptualization, Writing – review & editing, Supervision

Declaration of competing interest

The authors declare that they have no known competing financial interests or personal relationships that could have appeared to influence the work reported in this paper.

Acknowledgement

The authors gratefully acknowledge the support from the Research Council of Norway through the research project Understanding behaviour of district heating systems integrating distributed sources under the FRIPRO/FRINATEK program (project number 262707).

Appendix A. Parameters for the building model

Table A.1
Key parameters for the building model.

Category	Parameter	Value
Areas of building envelope (m^2)	Exterior wall	102,600
	Roof	75,400
	Ground floor	75,900
	Window	40,700
U-value of building envelope ($W/(m^2 \cdot K)$)	Exterior wall	0.48
	Roof	0.41
	Ground floor	0.17
	Window	2.07
Ventilation system	Air change rate (1/h)	2.45
	Heat recovery efficiency (%)	58
	Building air volume (m^3)	1,054,600

Appendix B. Parameters for the DC model

Table B.1
Key parameters for the heat pump component in the data centre model.

Category	Parameter	Value
Annual average conditions	Temperature difference on the evaporator/condensation side (K)	−4/12
	Nominal mass flow rate on the evaporator/condensation side (kg/s)	18/36
Baseline	Carnot effectiveness	0.4
Maximum capacity	Nominal compressor power (kW)	850

Appendix C. Parameters for the WT and BTES system model

Table C.1
Key parameters for the water tank model.

Parameter	Value
Height (m)	15
Volume (m^3)	8,000

Table C.2
Key parameters for the borehole thermal energy storage model.

Category	Parameter	Value
Bore field	Length/width (m)	69/27
	Number of boreholes	240
	Distance between two boreholes (m)	3
Borehole	Height (m)	55
	Radius (m)	0.063
Tube	Type	Single U
	Radius (m)	0.0167
	Thermal conductivity ($W/(m \cdot K)$)	0.39
	Thickness (m)	0.003
Filling material	Thermal conductivity ($W/(m \cdot K)$)	1.15
	Specific heat capacity ($J/(K \cdot kg)$)	800
	Density ($kg/(m^3)$)	1,600
Soil	Thermal conductivity ($W/(m \cdot K)$)	2.7 [63]
	Specific heat capacity ($J/(K \cdot kg)$)	840 [63,64]
	Density (kg/m^3)	2,800 [63,64]
	Temperature (°C)	5.0

Table C.3
Key parameters for the heat pump component in the borehole thermal energy storage system model.

Category	Parameter	Value
Annual average conditions	Temperature difference on the evaporator/condensation side (K)	−4/12
	Nominal mass flow rate on the evaporator/condensation side (kg/s)	14/28
Baseline	Carnot effectiveness	0.4
Maximum capacity	Nominal compressor power (kW)	680

Appendix D. Parameters for the MS model

Table D.1
Key parameters for the main substation model.

Parameter	Value
Heat transfer area (m^2)	420
Design capability (MW)	15.6

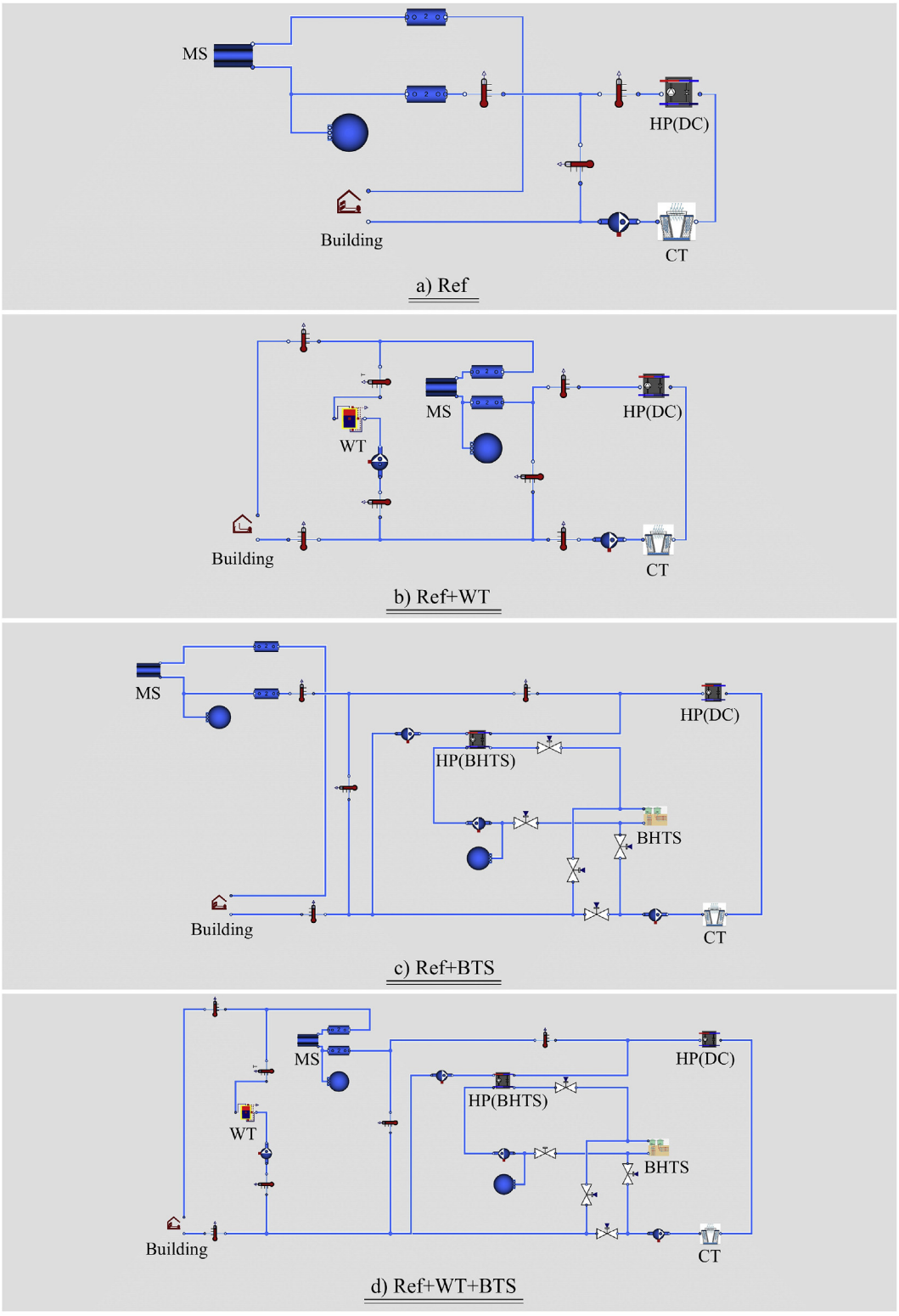

Fig. E1. Dymola models of the four scenarios.

References

[1] Frederiksen S, Werner S. District heating and cooling. Studentlitteratur Lund; 2013.
[2] Anderson A, Rezaie B. Geothermal technology: trends and potential role in a sustainable future. Appl Energy 2019;248:18–34.
[3] Holmgren K. Role of a district-heating network as a user of waste-heat supply from various sources – the case of Göteborg. Appl Energy 2006;83(12):1351–67.
[4] Li H, Nord N. Transition to the 4th generation district heating - possibilities, bottlenecks, and challenges. Energy Procedia 2018;149:483–98.

[5] Rezaie B, Rosen MA. District heating and cooling: review of technology and potential enhancements. Appl Energy 2012;93:2–10.
[6] Tian Z, Perers B, Furbo S, Fan J. Thermo-economic optimization of a hybrid solar district heating plant with flat plate collectors and parabolic trough collectors in series. Energy Convers Manag 2018;165:92–101.
[7] Tian Z, Zhang S, Deng J, Fan J, Huang J, Kong W, et al. Large-scale solar district heating plants in Danish smart thermal grid: developments and recent trends. Energy Convers Manag 2019;189:67–80.
[8] Tschopp D, Tian Z, Berberich M, Fan J, Perers B, Furbo S. Large-scale solar thermal systems in leading countries: a review and comparative study of Denmark, China, Germany and Austria. Appl Energy 2020;270:114997.
[9] Werner S. International review of district heating and cooling. Energy 2017;137:617–31.
[10] Lund H, Möller B, Mathiesen BV, Dyrelund A. The role of district heating in future renewable energy systems. Energy 2010;35(3):1381–90.
[11] Lund H, Østergaard PA, Chang M, Werner S, Svendsen S, Sorknæs P, et al. The status of 4th generation district heating: research and results. Energy 2018;164:147–59.
[12] Lund H, Werner S, Wiltshire R, Svendsen S, Thorsen JE, Hvelplund F, et al. 4th Generation District Heating (4GDH) Integrating smart thermal grids into future sustainable energy systems. Energy 2014;68:1–11.
[13] Upham P, Jones C. Don't lock me in: public opinion on the prospective use of waste process heat for district heating. Appl Energy 2012;89(1):21–9.
[14] Brand M, Svendsen S. Renewable-based low-temperature district heating for existing buildings in various stages of refurbishment. Energy 2013;62:311–9.
[15] Fang H, Xia J, Jiang Y. Key issues and solutions in a district heating system using low-grade industrial waste heat. Energy 2015;86:589–602.
[16] Koch K, Höfner P, Gaderer M. Techno-economic system comparison of a wood gas and a natural gas CHP plant in flexible district heating with a dynamic simulation model. Energy 2020;202:117710.
[17] Wahlroos M, Pärssinen M, Manner J, Syri S. Utilizing data center waste heat in district heating – impacts on energy efficiency and prospects for low-temperature district heating networks. Energy 2017;140:1228–38.
[18] Wahlroos M, Pärssinen M, Rinne S, Syri S, Manner J. Future views on waste heat utilization – case of data centers in Northern Europe. Renew Sustain Energy Rev 2018;82:1749–64.
[19] Koomey J. Growth in data center electricity use 2005 to 2010. 2011.
[20] Lu T, Lü X, Remes M, Viljanen M. Investigation of air management and energy performance in a data center in Finland: case study. Energy Build 2011;43(12):3360–72.
[21] Nadjahi C, Louahlia H, Lemasson S. A review of thermal management and innovative cooling strategies for data center. Sustainable Computing: Informatics and Systems 2018;19:14–28.
[22] Ebrahimi K, Jones GF, Fleischer AS. A review of data center cooling technology, operating conditions and the corresponding low-grade waste heat recovery opportunities. Renew Sustain Energy Rev 2014;31:622–38.
[23] Davies GF, Maidment GG, Tozer RM. Using data centres for combined heating and cooling: an investigation for London. Appl Therm Eng 2016;94:296–304.
[24] Kauko H, Kvalsvik KH, Rohde D, Nord N, Utne Å. Dynamic modeling of local district heating grids with prosumers: a case study for Norway. Energy 2018;151:261–71.
[25] Huang P, Copertaro B, Zhang X, Shen J, Löfgren I, Rönnelid M, et al. A review of data centers as prosumers in district energy systems: renewable energy integration and waste heat reuse for district heating. Appl Energy 2020;258:114109.
[26] Fiandrino C, Kliazovich D, Bouvry P, Zomaya AY. Performance and energy efficiency metrics for communication systems of cloud computing data centers. IEEE Transactions on Cloud Computing 2015;5(4):738–50.
[27] Noussan M, Jarre M, Poggio A. Real operation data analysis on district heating load patterns. Energy 2017;129:70–8.
[28] Shah SK, Aye L, Rismanchi B. Seasonal thermal energy storage system for cold climate zones: a review of recent developments. Renew Sustain Energy Rev 2018;97:38–49.
[29] Rohde D, Andresen T, Nord N. Analysis of an integrated heating and cooling system for a building complex with focus on long–term thermal storage. Appl Therm Eng 2018;145:791–803.
[30] Rohde D, Knudsen BR, Andresen T, Nord N. Dynamic optimization of control setpoints for an integrated heating and cooling system with thermal energy storages. Energy 2020;193:116771.
[31] Köfinger M, Schmidt RR, Basciotti D, Terreros O, Baldvinsson I, Mayrhofer J, et al. Simulation based evaluation of large scale waste heat utilization in urban district heating networks: optimized integration and operation of a seasonal storage. Energy 2018;159:1161–74.
[32] Moser S, Mayrhofer J, Schmidt R-R, Tichler R. Socioeconomic cost-benefit-analysis of seasonal heat storages in district heating systems with industrial waste heat integration. Energy 2018;160:868–74.
[33] Song J, Wallin F, Li H. District heating cost fluctuation caused by price model shift. Appl Energy 2017;194:715–24.
[34] Larsson O. Pricing models in district heating. 2011.
[35] Sjödin J, Henning D. Calculating the marginal costs of a district-heating utility. Appl Energy 2004;78(1):1–18.
[36] Liu W, Klip D, Zappa W, Jelles S, Kramer GJ, van den Broek M. The marginal-cost pricing for a competitive wholesale district heating market: a case study in The Netherlands. Energy 2019;189:116367.
[37] Björkqvist O, Idefeldt J, Larsson A. Risk assessment of new pricing strategies in the district heating market: a case study at Sundsvall Energi AB. Energy Policy 2010;38(5):2171–8.
[38] Verda V, Colella F. Primary energy savings through thermal storage in district heating networks. Energy 2011;36(7):4278–86.
[39] Harris M. Thermal energy storage in Sweden and Denmark: potentials for technology transfer. IIIEE Master thesis; 2011.
[40] Verrilli F, Srinivasan S, Gambino G, Canelli M, Himanka M, Del Vecchio C, et al. Model predictive control-based optimal operations of district heating system with thermal energy storage and flexible loads. IEEE Trans Autom Sci Eng 2017;14(2):547–57.
[41] Jebamalai JM, Marlein K, Laverge J. Influence of centralized and distributed thermal energy storage on district heating network design. Energy 2020;202:117689.
[42] Guan J, Nord N, Chen S. Energy planning of university campus building complex: energy usage and coincidental analysis of individual buildings with a case study. Energy Build 2016;124:99–111.
[43] Nord N, Sandberg NH, Ngo H, Nesgård E, Woszczek A, Tereshchenko T, et al. Future energy pathways for a university campus considering possibilities for energy efficiency improvements. Conference Future energy pathways for a university campus considering possibilities for energy efficiency improvements, vol. vol. 352. IOP Publishing, p. 12037.
[44] Lu Y. Design handbook for HVAC system (in Chinese). China Architecture & Building Press; 2007.
[45] Zuo W, Nouidui TS, Pang X. Modelica buildings library. Journal of Building Performance Simulation 2014;7(4):253–70.
[46] Buildings.ThermalZones.ReducedOrder.RC. https://simulationresearch.lbl.gov/modelica/releases/latest/help/Buildings_ThermalZones_ReducedOrder_RC.html#Buildings.ThermalZones.ReducedOrder.RC.TwoElements; 2020.
[47] Modelica standard library. https://github.com/modelica/ModelicaStandardLibrary; 2020.
[48] IBPSA project 1. https://ibpsa.github.io/project1/index.html; 2020.
[49] Reynders G, Baetens R, Picard D, Saelens D, Helsen L. Implementation and verification of the IDEAS building energy simulation library. Journal of Building Performance Simulation 2018;11(6):669–88.
[50] Annex60.Fluid.HeatPumps. 2020. http://www.iea-annex60.org/releases/modelica/1.0.0/help/Annex60_Fluid_HeatPumps.html#Annex60.Fluid.HeatPumps.Carnot_y. last accessed in December 2020.
[51] Modelica AixLib library. 2020. https://github.com/modelica-3rdparty/AixLib.
[52] AixLib.Fluid.Storage.UsersGuide. 2020. https://build.openmodelica.org/Documentation/AixLib.Fluid.Storage.UsersGuide.html. last accessed in December 2020.
[53] IBPSA.Fluid.Geothermal.Borefields.UsersGuide. 2020. https://build.openmodelica.org/Documentation/IBPSA.Fluid.Geothermal.Borefields.UsersGuide.html. last accessed in December 2020.
[54] Modelica.Fluid.Examples.HeatExchanger.BaseClasses.BasicHX. 2020. https://www.maplesoft.com/documentation_center/online_manuals/modelica/Modelica_Fluid_Examples_HeatExchanger_BaseClasses.html.
[55] Mangold D, Deschaintre L. Task 45 Large Systems Seasonal thermal energy storage Report on state of the art and necessary further R+ D. International Energy Agency Solar Heating and Cooling Programme. 2015.
[56] Clausen KS, From N, Hofmeister M, Paaske BL, Flørning J. Large heat pump projects in the district heating system (in Danish). Copenhagen: Danish Energy Agency; 2014.
[57] Statkraft Varme at tronheim. 2020. https://www.statkraftvarme.no/om-statkraftvarme/vare-anlegg/norge/trondheim/.
[58] Heating price at tronheim. https://www.statkraftvarme.no/globalassets/2-statkraft-varme/statkraft-varme-norge/om-statkraft-varme/prisark/20190901/fjernvarmetariff-trondheim-bt1.pdf; 2020.
[59] Jaluria Y. Design and optimization of thermal systems. CRC press; 2007.
[60] The policy rate. https://www.norges-bank.no/en/topics/Monetary-policy/Policy-rate/; 2020.
[61] CO_2 and greenhouse gas emissions. https://ourworldindata.org/co2-and-other-greenhouse-gas-emissions#global-warming-to-date; 2020.
[62] Electricity disclosure 2018. https://www.nve.no/norwegian-energy-regulatory-authority/retail-market/electricity-disclosure-2018/; 2020.
[63] Liebel HT. Influence of groundwater on measurements of thermal properties in fractured aquifers. 2012.
[64] Sibbet B, McClenahan D. Seasonal borehole thermal energy storage—guidelines for design & construction. Denmark: Natural Resources: Hvalsoe; 2015.